BJP British Journal of Pharmacology

DOI:10.1111/bph.12745
www.brjpharmacol.org

RESEARCH PAPER

The effect of hyperpolarization-activated cyclic nucleotide-gated ion channel inhibitors on the vagal control of guinea pig airway smooth muscle tone

Alice E McGovern, Jed Robusto, Joanna Rakoczy, David G Simmons, Simon Phipps and Stuart B Mazzone

School of Biomedical Sciences, University of Queensland, St Lucia, Qld, Australia

Correspondence
Stuart B Mazzone, School of Biomedical Sciences, University of Queensland, St Lucia, Qld 4072, Australia. E-mail: s.mazzone@uq.edu.au

Received
27 August 2013
Revised
10 February 2014
Accepted
14 February 2014

BACKGROUND AND PURPOSE

Subtypes of the hyperpolarization-activated cyclic nucleotide-gated (HCN) family of cation channels are widely expressed on nerves and smooth muscle cells in many organ systems, where they serve to regulate membrane excitability. Here we have assessed whether HCN channel inhibitors alter the function of airway smooth muscle or the neurons that regulate airway smooth muscle tone.

EXPERIMENTAL APPROACH

The effects of the HCN channel inhibitors ZD7288, zatebradine and Cs^+ were assessed on agonist and nerve stimulation-evoked changes in guinea pig airway smooth muscle tone using tracheal strips *in vitro*, an innervated tracheal tube preparation *ex vivo* or in anaesthetized mechanically ventilated guinea pigs *in vivo*. HCN channel expression in airway nerves was assessed using immunohistochemistry, PCR and *in situ* hybridization.

KEY RESULTS

HCN channel inhibition did not alter airway smooth muscle reactivity *in vitro* to exogenously administered smooth muscle spasmogens, but significantly potentiated smooth muscle contraction evoked by the sensory nerve stimulant capsaicin and electrical field stimulation of parasympathetic cholinergic postganglionic neurons. Sensory nerve hyperresponsiveness was also evident in *in vivo* following HCN channel blockade. Cs^+, but not ZD7288, potentiated preganglionic nerve-dependent airway contractions and over time induced autorhythmic preganglionic nerve activity, which was not mimicked by inhibitors of potassium channels. HCN channel expression was most evident in vagal sensory ganglia and airway nerve fibres.

CONCLUSIONS AND IMPLICATIONS

HCN channel inhibitors had a previously unrecognized effect on the neural regulation of airway smooth muscle tone, which may have implications for some patients receiving HCN channel inhibitors for therapeutic purposes.

Abbreviations

4-AP, 4-aminopyridine; $ED_{50}/EF_{50}/EV_{50}$, voltage/frequency producing 50% of the maximal response; EFS, electrical field stimulation; HCN, hyperpolarization-activated cyclic nucleotide-gated; I_h, hyperpolarization-activated inward depolarizing current; MEM, minimum essential media; NK, neurokinin; PIP, pulmonary inflation pressure; TEA, triethylammonium chloride; TTX, tetrodotoxin

Introduction

In many species, including humans, vagal parasympathetic pathways mediate both cholinergic contractions and non-cholinergic relaxations of the airways (the latter mediated by the gaseous transmitter NO and vasoactive intestinal peptide) (e.g. Belvisi *et al.*, 1992; Canning and Undem, 1993; reviewed in Canning, 2006). In some species (but not humans), the sympathetic nervous system may also provide direct relaxant (adrenergic) innervation to airway smooth muscle (Richardson and Béland, 1976; Oh *et al.*, 2006). Preganglionic neuronal activity arising from the CNS is subject to varying degrees of processing at the level of the airway parasympathetic ganglia (Myers *et al.*, 1990; Myers and Undem, 1991). In addition to preganglionic input, parasympathetic ganglia associated with the airways may also receive inputs from other airway ganglia, airway sensory neurons and a variety of locally produced or circulating chemical substances (Myers *et al.*, 1991; Myers and Undem, 1993; Mazzone and McGovern, 2010). Furthermore, pulmonary sensory nerves can reflexively regulate autonomic outflow to the airways via the CNS and, in some species, mediate the contraction of airway smooth muscle via axon reflexes (Mazzone and Canning, 2002a,b). Collectively, these neural pathways all help shape the final signal that is transmitted to the airway smooth muscle, and hence their ongoing activity is largely responsible for establishing the degree of baseline airway obstruction in both health and disease. With this in mind, understanding the mechanisms that regulate preganglionic, postganglionic and sensory neural activity may have important implications for understanding the symptoms that accompany many airway diseases.

Hyperpolarization-activated cyclic nucleotide-gated (HCN) ion channels are a class of voltage-gated cation channel that are expressed by a variety of excitable cells (see Alexander *et al.*, 2013). Four HCN channel subtypes have been identified, and all carry a slowly developing inward depolarizing (mostly Na^+) current termed I_h at progressively larger hyperpolarized membrane potentials or in the presence of cyclic nucleotides (e.g. cAMP). Because these channels are activated near the resting membrane potential, I_h therefore plays an important role in regulating cell excitability (Doan *et al.*, 2004; Biel *et al.*, 2009; Zhou *et al.*, 2010). Perhaps the most familiar example of this is in cardiac muscle sinoatrial nodal cells where HCN4 is involved in the 'pacemaker current' responsible for setting basal cardiac rhythm (Nof *et al.*, 2010). In the nervous system, however, HCN channels are expressed by a wide variety of peripheral and central neurons where they play quite diverse roles in regulating excitability and neuronal firing depending on the channel subtype and neuron in question.

Electrophysiological and expression data are consistent with a role for HCN channels in the regulation of vagal sensory and motor neurons. For example, all of the HCN channel subtypes have been detected in the vagal sensory ganglia or on vagal nerve terminals in peripheral tissues (Doan *et al.*, 2004; Tu *et al.*, 2010; Liu *et al.*, 2012). Blockade of I_h with millimolar concentrations of caesium ions (Cs^+) or the selective channel inhibitor ZD7288 has been reported to both increase and decrease vagal sensory neuron excitability; its effect perhaps depending on the specific channel or neuronal subpopulation being studied (Doan *et al.*, 2004; Zhou *et al.*, 2010). Similarly, I_h currents have been demonstrated in some nucleus ambiguus neurons in the brainstem (where many vagal preganglionic neurons originate) and in neurons of several peripheral autonomic ganglia (Vanner *et al.*, 1993; Nishimura *et al.*, 1995; Lamas, 1998; Tompkins *et al.*, 2009). However, to date there have been no studies specifically investigating whether HCN channels on vagal neurons contribute to the control of bronchomotor tone. Therefore in this study, we set out to assess the effects of the HCN channel blocking agents Cs^+, ZD7288 and zatebradine on vagal preganglionic, postganglionic and sensory nerve-dependent regulation of airway smooth muscle tone and to determine whether HCN channels are expressed by neuronal populations innervating the airways.

Methods

All experiments conducted in this study were approved by an accredited institutional Animal Ethics Committee. Experiments were performed on male Hartley guinea pigs (300–400 g, n = 130; IMVS, Adelaide, SA, Australia). All studies involving animals are reported in accordance with the ARRIVE guidelines for reporting experiments involving animals (Kilkenny *et al.*, 2010; McGrath *et al.*, 2010).

Experiments using guinea pig tracheal strips in vitro

Guinea pigs were killed with an overdose of sodium pentobarbital (Lethabarb, Virbac Pty Ltd, Milperra, NSW, Australia), and the entire trachea (from the first cartilage ring to the carina) was rapidly removed and placed in warmed (37°C), oxygenated Krebs bicarbonate buffer (Sigma, Sydney, NSW, Australia) [composition (mM) NaCl (118), KCl (5.4), $NaHPO_4$ (1), $MgSO_4$ (1.2), $CaCl_2$ (1.9), $NaHCO_3$ (25) and dextrose (11.1)]. Three micromolar of indomethacin and 2 μM of propranolol were added to the buffer in all experiments to prevent any confounding effects of prostaglandins or catecholamines (Mazzone and Canning, 2002c). Tracheal strips, each two cartilage rings in length, were prepared and suspended under 1.5 g of passive isometric tension between custom-built bipolar platinum ring electrodes in 10 mL organ baths and equilibrated for 1 h by washing four times with fresh Krebs bicarbonate buffer. Tracheal tension was measured isometrically using calibrated force transducers; the output from which was digitized and displayed on a desktop personal computer running LabScribe software (iWorx Systems Inc, Dover, NH, USA).

Initial experiments assessed whether CsCl (10 μM–100 mM), ZD7288 (0.1–100 μM) or zatebradine (10 nM–10 μM) exhibited any direct airway smooth muscle contractile effects. Subsequent experiments compared the effects of 5 mM CsCl, 60 μM ZD7288 or 4 μM zatebradine on dose-dependent contractions evoked by bath application of (i) the muscarinic cholinergic agonist carbachol (10 pM–10 μM); (ii) histamine (100 pM–1 mM); (iii) the selective neurokinin (NK) 2 receptor agonist Nle^{10}-$NKA_{(4-10)}$ (100 pM–1 mM); or (iv) the sensory C-fibre stimulant capsaicin (1 nM–10 μM). HCN channel blocking treatments were administered for 60 min before the first dose of contractile agonist was added and subsequent doses of agonist were only administered once contractions

evoked by the previous dose had reach a stable maximum. In additional experiments, contractions and relaxations evoked by electrical field stimulation (EFS; Grass Model S44 stimulator, Grass Technologies, Warwick, RI, USA) of tracheal strips were performed in the presence and absence of HCN channel inhibitors. Initially, voltage–response curves for contractions and relaxations were assessed (1 ms pulse duration, 32 Hz, 10 s trains) following which frequency–response curves were assessed at optimum stimulating voltages (typically 50–60 V). EFS-evoked relaxations were studied following addition of atropine (1 μM) and contraction of the trachealis with histamine (10 μM). Where stated the following additional treatments were used: hexamethonium chloride (100 μM) was used to prevent ganglionic transmission (i.e. between preganglionic and postganglion neurons), atropine (1 μM) was used to inhibit muscarinic cholinoceptors on the airway smooth muscle, the combination of CP99994/SR48968/SB222200 (0.1 μM each) was used to block the smooth muscle and/or ganglionic effects of endogenously released (from C-fibres) NKs acting at NK_1/NK_2/NK_3 receptors (Mazzone and Canning, 2002c), and pyrilamine maleate (1 μM) was used to block histamine H_1 receptors.

At the end of all experiments, the maximum attainable contraction of the trachea was determined by adding $BaCl_2$ (300 mM) to the buffer. Contractions were expressed as a % of the maximum contraction, whereas relaxations were expressed as % reversal of the histamine-induced contractions. Numerical data were tabulated in GraphPad Prism (version 6.01; Graphpad software, San Diego, CA, USA), plotted and a non-linear agonist–response curve fitted. Data are presented as mean ± SEM and where appropriate effective concentrations/voltages/frequencies producing 50% of the maximum (EC_{50}, EV_{50} and EF_{50}, respectively) were obtained from estimates provided by GraphPad Prism.

Experiments using an innervated guinea pig trachea tube in vitro

Vagus nerve-dependent contractions of the guinea pig trachea were measured using an *in vitro* innervated tracheal tube preparation similar to that described previously (Canning and Undem, 1993). Briefly, guinea pigs were killed with sodium pentobarbital and exsanguinated. The trachea, adjacent oesophagus and extrinsic (vagus) nerves were removed *en bloc* and pinned to the base of a sylgard-lined water-jacketed dissection dish that was continuously overfilled with warmed (37°C), oxygenated Krebs bicarbonate buffer containing 3 μM indomethacin (as above). The trachea and associated nerves were then cleaned of any excess connective tissue ensuring not to damage any of the extrinsic neural innervation. Two lengths of suture were tied opposite each other on the lateral aspects of the trachea onto cartilage rings 6 and 7 caudal to the larynx. One suture was anchored to the bath with dissecting pins while the other was secured to an isometric force transducer (model FT03C; Grass Instruments, Quincy, MA, USA), the output of which was amplified and filtered (NeuroLog System; Digitimer, Hertfordshire, UK), digitized (Micro1401 A–D converter; CED, Cambridge, UK) and recorded using Spike II software (CED). Optimal baseline tension was set (1.5–2 g) and maintained throughout the equilibration period. The vagi were placed on a custom-made silver wire hook electrode (for vagus nerve stimulation) and a custom-made bipolar stainless steel field-stimulating electrode was positioned either side of the tracheal tube (for EFS-evoked contractions). Thirty minutes before the start of each experiment 2 μM propranolol and 0.1 μM each of CP99994/SR48968/SB222200 were added to the perfusion buffer as described above.

For vagally mediated contractions, voltage- and frequency–response curves (1 ms pulses, 10 s trains) were compared in the absence and presence of Cs^+ (5 mM) or ZD7288 (60 μM). Treatments were given 20 min before the first vagus nerve stimulus. For field stimulation experiments, the voltage producing 50% of the maximum EFS-evoked contraction (defined as the EV_{50}, at 32 Hz, 1 ms pulses, 10 s trains) was first determined and then this stimulus was repeatedly delivered (180 s inter-train interval) until contraction peaks were stable (i.e. of consistent magnitude) at which point tissues were treated with the following: (i) 5 mM Cs^+; (ii) 60 μM ZD7288; (iii) 100 nM iberiotoxin; (iv) 100 μM 4-aminopyridine (4-AP); (v) 2 mM triethylammonium chloride (TEA); (vi) 100 nM–1 μM apamin. In experiments employing Cs^+, tissues were also treated with 1 μM tetrodotoxin (TTX), 100 μM hexamethonium and/or 1 μM atropine 60 min after the addition of Cs^+. At the end of all experiments, the maximum attainable contraction of the trachea was determined by adding 300 mM $BaCl_2$ to the buffer, and data were analysed as detailed above.

Organotypic tissue cultures

Organotypic cultures of the guinea pig trachea were carried out to remove the extrinsic neural innervation as previously described (Mazzone and McGovern, 2010). Guinea pigs were deeply anaesthetized with sodium pentobarbital (100 $mg \cdot kg^{-1}$ i.p.) and transcardially perfused with 500 mL of sterile 10 mM PBS. The trachea was removed (dissected free from the oesophagus) and quickly submerged in cold, sterile minimum essential media (MEM) with Earle's salts and L-glutamine (Sigma). Care was taken to remove all excess connective tissue and all extrinsic nerves. Tracheae were cultured for 48 h at 37°C in sterile, carbogen gassed MEM containing 10 μM indomethacin, 20 $U \cdot mL^{-1}$ penicillin and 20 $\mu g \cdot mL^{-1}$ streptomycin (Sigma). The culture media were changed every 12 h, and after 48 h tracheal strips or whole tracheal tubes were prepared for EFS-evoked contraction studies as described above.

In vivo *measurements of pulmonary insufflation pressures in anaesthetized guinea pigs*

Guinea pigs (n = 35) were anaesthetized with 1–1.5 $g \cdot kg^{-1}$ urethane (i.p.) and positioned supine on a heated pad. Induction of a surgical plane of anaesthesia was assessed initially by testing corneal reflexes and head shake reactions and then monitored throughout the experiment by assessing blood pressure responses to noxious stimulation of the skin. The extrathoracic trachea was exposed via a midline incision on the ventral surface of the neck the caudal most portion of the trachea was cannulated with a 16G Luer-Stub (Harvard Apparatus, Holliston, MA, USA). The animals were mechanically ventilated (60 breaths min^{-1}, 6 $mL \cdot kg^{-1}$, 2–3 cm H_2O of positive end-expiratory pressure) following paralysis (2 $mg \cdot kg^{-1}$ succinylcholine chloride s.c.) as previously described

(Mazzone and Canning, 2002c). Pulmonary inflation pressure (PIP) was measured via a pressure transducer attached to a side port of the ventilation circuit. The abdominal aorta and vena cava were cannulated to monitor arterial blood pressure and for i.v. drug injection respectively. Physiological measures were amplified and filtered (NeuroLog System; Digitimer), digitized (Micro1401 A–D converter; CED) and recorded using Spike II software (CED). Instantaneous heart rate was calculated from the recorded arterial pressure signal. After completion of surgeries, all animals were treated with an i.v. injection of propranolol HCl (2 mg·kg^{-1} in sterile saline). Some animals (where indicated) also received 2 mg·kg^{-1} ZD7288 and/or 0.3 mg·kg^{-1} of each of the NK antagonists CP99994/SR48968. All animals were then allowed to stabilize for 20 min before continuing with the experiment.

Increases in PIP were measured in response to i.v. administered histamine (0.05 ml of 0.5–20 μg·kg^{-1}) or capsaicin (0.05 ml of 0.5–40 mg·kg^{-1}). Each i.v. drug injection was followed immediately by a 0.1 ml saline flush of the cannula, and artificial sighs (volume histories) were delivered before all challenges by means of clamping the expiratory port of the ventilator. Stimulus-induced changes in PIP were expressed as % change relative to the baseline PIP. At the conclusion of each experiment, animals were killed by an i.v. injection of sodium pentobarbital.

Immunohistochemistry

Immunohistochemical staining of airway and neural tissues was performed to assess the expression of specific HCN channel subtypes. In initial experiments we assessed tissues harvested from guinea pigs, but found that the commercially obtained HCN antisera employed were unreliable in this species (data not shown). We therefore opted to use rat tissues, a species in which these antisera had been previously used successfully. Briefly, animals were deeply anaesthetized with sodium pentobarbital (100 mg·kg^{-1}) and transcardially perfused with 10 mM PBS followed by 4% paraformaldehyde. Nodose and jugular ganglia, brainstem and trachea were removed for further immunohistochemical processing. Ganglia and brainstem were rapidly frozen in optimal cutting temperature compound and cut (12 μm for ganglia or 50 μm for brainstem) using a cryostat. Sections (slide-mounted sections for ganglia and free floating for brainstem) were incubated for 1 h in blocking solution (PBS, 10% goat serum) and then overnight (at room temperature) with rabbit anti-HCN1-4 antisera (1:200; Abcam, Cambridge, MA, USA). Staining was detected with Alexa Fluor 488 (Life Technologies, Mulgrave, Vic., Australia) or 594-conjugated goat anti-rabbit IgG (1:500; Molecular Probes, Inc., Eugene, OR, USA) and visualized using an Olympus BX51 microscope (Olympus, Notting Hill, Vic., Australia) equipped with an Optronics digital camera (Olympus). Trachea were prepared as whole-mounts, as previously described (Mazzone and McGovern, 2010) and processed for immunohistochemical staining as described above for tissue sections. Negative control experiments, in which the primary antibody was replaced with non-immune serum, were conducted where appropriate.

Reverse transcriptase PCR

Guinea pigs ($n = 2$) were overdosed with sodium pentobarbital (100 mg·kg^{-1}) and vagal ganglia (jugular and nodose), brainstem (at the level of the rostral nucleus ambiguus), lung and trachealis muscle were rapidly removed and snap frozen. Tissues were homogenized and RNA was extracted using the RNeasy mini kit (Qiagen, Chadstone, Vic., Australia) with purified RNA reversed transcribed to cDNA using BioScript reverse transcriptase (Bioline, Alexandria, NSW, Australia) following the manufacturer's instructions. The PCR reaction contained 1 U of Hot Start MyTaq Polymerase (Bioline), with PCR buffer, template cDNA and primer pairs for β-actin and HCN1-4 based on the predicted guinea pig β-actin and HCN1-4 mRNA transcripts: β-actin forward 5′ GGACTTC GAGCAGGAGATGG 3′, reverse 5′ CCTAGAGCATTTGCG GTGC 3′; HCN1 forward 5′ GCGGCAATACCAAGAGAAGT 3′, reverse 5′ CTCCCTGTCGTGTTTCACAA 3′; HCN2 forward 5′ GCTTCACCAAGATCCTCAGC 3′, reverse 5′ GCTGGAAG ACCTCGAACTTG; HCN3 forward 5′ CCAAGCTACGCTT TGAGGTC 3′, reverse 5′ GAAGGTGGCTGGAGAGTCAG 3′; HCN4 forward 5′ CAGCGCATCCACGACTACTA 3′, reverse 5′ GTCATGCTGCACAATCTGCT 3′. The PCR conditions included 35 cycles with initial denaturation at 98°C for 1 min, denaturation at 98°C for 10 s, annealing at 58°C (HCN2 62°C) for 15 s, extension at 72°C for 30 s, followed by a final extension at 72°C for 5 min. Products were visualized by electrophoresis on ethidium bromide stained 1.5% agarose gels.

In situ *hybridization*

cDNA probes for HCN1, HCN2, HCN3 and HCN4 were generated by RT-PCR. Amplicons were cloned into pGEM-T Easy (Promega, Alexandria, NSW, Australia) and verified by sequencing. Digoxigenin (DIG) probes were generated from plasmids following the manufacturer's instructions (DIG RNA Labeling Mix Cat. 11277073910; Roche, Castle Hill, NSW, Australia). Tissues (nodose and jugular ganglia) used for *in situ* hybridization were dissected into 4% paraformaldehyde in PBS and fixed overnight at 4°C. Samples were processed, embedded in paraffin, sectioned at 5 μm before being dewaxed in xylene and rehydrated through an ethanol gradient to PBS under RNase-free conditions. Sections were treated with 30 μg·mL^{-1} proteinase K (Roche) in 50 mM Tris/ 2.5 mM EDTA for 20 min at room temperature, acetylated with 0.25% acetic anhydride (Sigma) in 0.1 M triethanolamine (Sigma) buffer for 10 min and hybridized with ~50 ng of DIG-labelled riboprobe/section [in 200 μL hybridization buffer; 1× salts (200 mM sodium chloride, 13 mM Tris, 5 mM sodium phosphate monobasic, 5 mM sodium phosphate dibasic, 5 mM EDTA), 50% formamide, 10% dextran-sulfate, 1 mg·mL^{-1} yeast tRNA (Roche), 1× Denhardt's (1% w v^{-1} BSA, 1% w v^{-1} Ficoll, 1% w v^{-1} polyvinylpyrrolidone)] at 65°C overnight. Posthybridization washes, antibody detection of DIG-labelled probes and colour development were all performed as previously described (Simmons *et al.*, 2008).

Data analysis and statistical procedures

Numerical data were tabulated in GraphPad Prism (version 6.01). Stimulus response results were plotted and a non-linear agonist response curve fitted. Data are presented as mean ± SEM and where appropriate effective concentrations/ doses/ voltages/ frequencies producing 50 % of the maximum (EC_{50}, ED_{50}, EV_{50} and EF_{50}, respectively) were obtained from estimates provided by GraphPad Prism. Differences between cal-

culated EC_{50}, ED_{50}, EV_{50} and EF_{50} values were assessed using a one way ANOVA followed by Tukey's multiple comparisons test. Blood pressure and heart rate responses were compared before and after drug administration using a paired *t*-test. In all instances $P < 0.05$ was considered significant.

Drugs and reagents

Apamin, 4-AP, atropine sulfate, barium chloride, capsaicin, heparin sulfate, hexamethonium, histamine, iberiotoxin, indomethacin, *dl*-propranolol hydrochloride, pyrilamine, succinylcholine chloride, TEA, urethane (ethyl carbamate), zatebradine and ZD7288 were purchased from Sigma (St. Louis, MO, USA). CP99994/SR48968/SB222200 were generous gifts from GlaxoSmithKline (King of Prussia, PA, USA). Stock solutions (10–20 mM) of all drugs added to Krebs buffer for *in vitro* experiments were made in distilled water except indomethacin (30 mM), capsaicin (10 mM) were dissolved in absolute ethanol, and CP99994/SR48968/SB222200 were dissolved (10 mM) in DMSO. Drugs administered i.v. or s.c. (1–50 mg·mL^{-1}) were dissolved in saline, except capsaicin that was dissolved in 10% ethanol/10% Tween 20/80% saline (Sigma).

Results

Effect of HCN channel inhibitors on airway smooth muscle

Cs^+ (2–5 mM), ZD7288 (10–100 μM) and zatebradine (2–50 μM) are commonly used to inhibit I_h (Marshall *et al.*, 1993; Doan *et al.*, 2004; Stieber *et al.*, 2005; 2006). We therefore first assessed the effect of these compounds on resting smooth muscle tone *in vitro* (Figure 1). Tracheal strips, in the presence of indomethacin (to inhibit prostaglandins), propranolol (to block β-adrenoceptors) and CP99994/SR48968/SB220000 (to inhibit NKs), dose-dependently contracted in response to both Cs^+ and zatebradine, but not ZD7288. Contractions in response to Cs^+ were slow in onset, and only occurred at a concentration of 10 mM or above (NB: subsequent experiments employed 5 mM Cs^+ to inhibit HCN channels and although this concentration was not specifically tested in the dose–response experiments shown in Figure 1, in >40 subsequent experiments 5 mM Cs^+ was without any direct effect on baseline smooth muscle tone). To assess whether Cs^+-evoked tracheal contractions were due to the endogenous release of ACh we repeated experiments in the presence of 1 μM atropine to block smooth muscle muscarinic receptors, and this failed to prevent the response (Figure 1A). No further characterization of the Cs^+ contractile response was performed. In contrast to Cs^+, zatebradine-evoked tracheal contractions at drug concentrations reportedly selective for HCN channels (i.e. contraction occurred between 1 and 10 μM zatebradine). Atropine produced negligible inhibition, whereas pretreatment with the histamine H_1 receptor antagonist pyrilamine completely abolished (and reversed, not shown) zatebradine-evoked responses. Because of the histamine-mimetic effect of zatebradine we conducted fewer overall experiments using this agent, and (when used) we included 1 μM pyrilamine in the experiment to limit this off-target effect.

In subsequent experiments, the effects of HCN channel inhibitors on tracheal contractions evoked by airway smooth muscle spasmogens was assessed (Figure 2; Table 1). The cholinergic agonist carbachol produced a dose-dependent increase in tracheal tension that was unaffected by Cs^+, ZD7288 or zatebradine. Similarly, HCN channel inhibition with ZD7288 failed to affect tracheal contractions evoked by histamine or the NK_2 receptor agonist $Nle^{10}NKA_{(4-10)}$. By contrast, contractile responses evoked by bath application of the sensory nerve stimulant capsaicin, which constricts airway smooth muscle by releasing neuropeptides (NKs) from C-fibre terminals in the airways, were significantly potentiated (leftward shift in the capsaicin dose–response curve) by both ZD7288 and Cs^+ (Figure 2F; Table 1).

Effect of HCN channel inhibitors on parasympathetic nerve-dependent responses

EFS of tracheal strips evokes neurally mediated contractions and relaxations of airway tissues, which are not dependent on ganglionic transmission. That is, EFS-evoked responses result

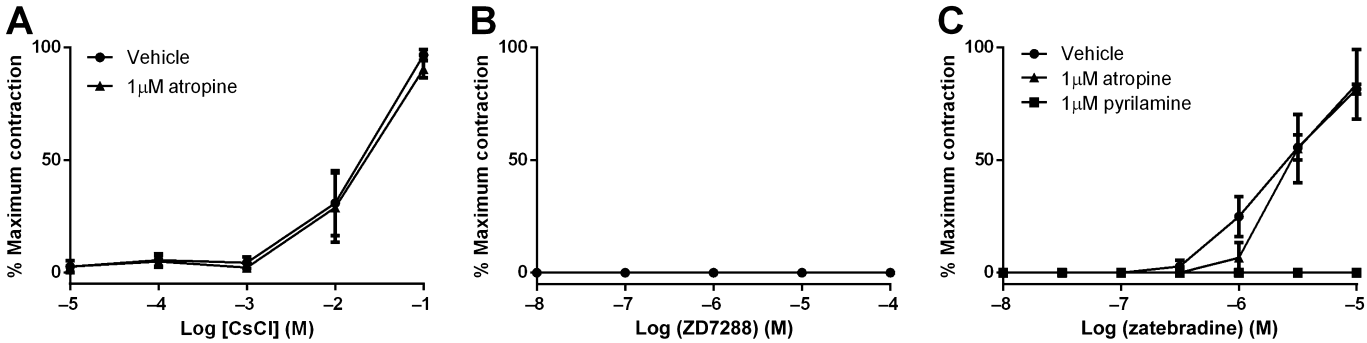

Figure 1

Effect of HCN channel inhibitors on airway smooth muscle tension *in vitro*. Tracheal strips were exposed to increasing concentrations of (A) CsCl, (B) ZD7288 or (C) zatebradine, and resulting changes in isometric smooth muscle tension recorded. Some tissues were pretreated with the muscarinic cholinergic receptor antagonist atropine (1 μM) or the histamine H_1 receptor antagonist pyrilamine (1 μM). Each graph represents the mean ± SEM of four experiments. See Methods for additional details. Inhibitor concentrations were chosen based on previous studies reporting their potency at HCN channels (e.g. see Marshall *et al.*, 1993; Doan *et al.*, 2004; Stieber *et al.*, 2005; 2006).

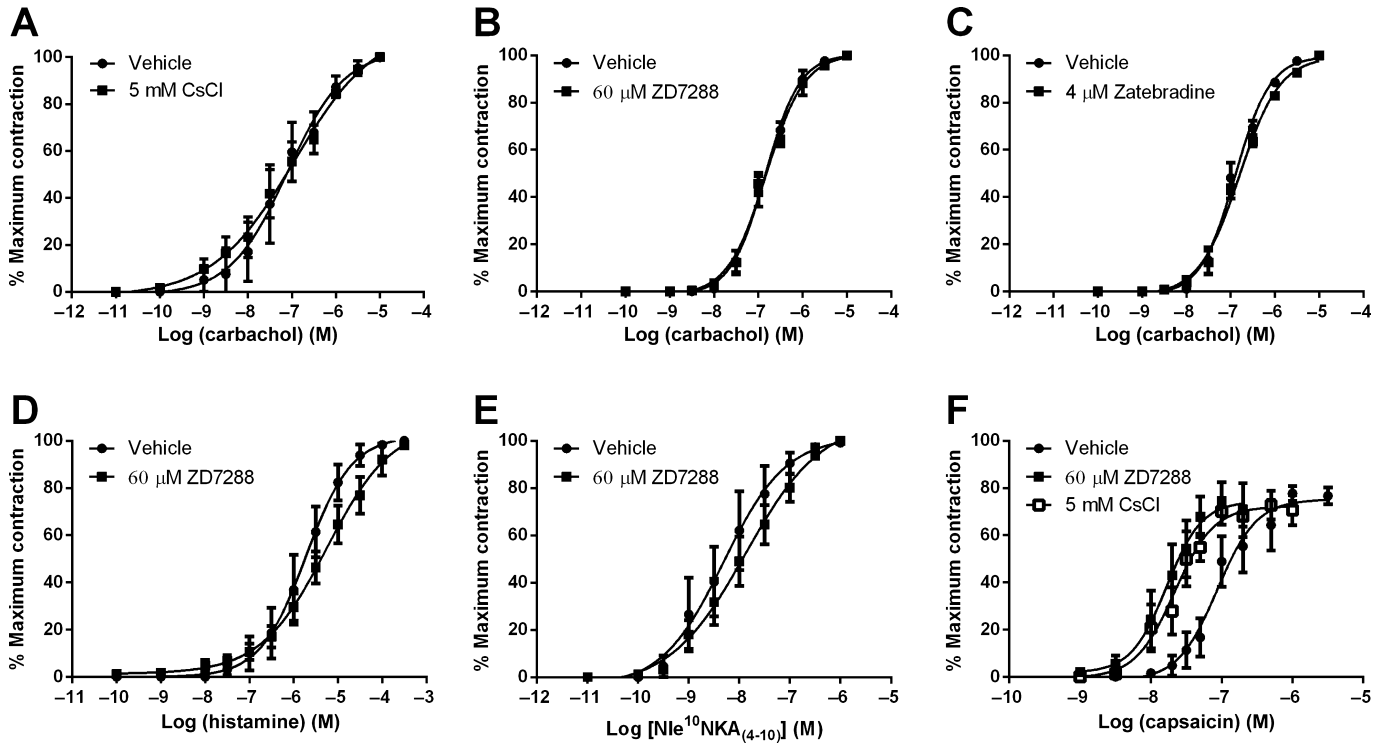

Figure 2

Effect of HCN channel inhibitors on responsiveness to agonist-evoked airway smooth muscle contractions *in vitro*. Tracheal strips were exposed to increasing concentrations of (A–C) the muscarinic cholinoceptor agonist carbachol, (D) histamine, (E) the NK receptor agonist Nle^{10}-$NKA_{(4–10)}$ or (F) the sensory nerve stimulant capsaicin, in the absence or presence of CsCl, ZD7288 or zatebradine. Each graph represents the mean ± SEM of four to eight experiments. See Methods for additional details and Table 1 for EC_{50} values.

Table 1

Effect of HCN channel inhibitors on agonist and nerve-evoked bronchoconstriction *in vitro*

	Treatment			
	Vehicle	**CsCl**	**ZD7288**	**Zatebradine**
Agonist[a]				
Carbachol (n = 4)	–6.93 ± 0.21	–7.05 ± 0.17	–6.85 ± 0.17	–6.72 ± 0.18
Histamine (n = 4)	–5.51 ± 0.26	ND	–5.18 ± 0.13	ND
Nle^{10}-$NKA_{(4–10)}$ (n = 4)	–8.02 ± 0.19	ND	–7.89 ± 0.26	ND
Capsaicin (n = 8)	–6.90 ± 0.07	–7.72 ± 0.09**	–7.81 ± 0.08**	ND
Electric field stimulation[b]				
Voltage (n = 6)	27.33 ± 1.56	21.46 ± 1.54*	26.36 ± 1.59	28.19 ± 1.45
Frequency (n = 6)	11.30 ± 2.10	3.95 ± 0.55*	2.06 ± 0.32**	10.61 ± 2.01
Frequency + culture (n = 4)	8.19 ± 2.61	3.87 ± 0.42*	ND	ND
Vagus nerve stimulation[b]				
Voltage (n = 6)	3.07 ± 0.36	2.68 ± 0.33	ND	ND
Frequency (n = 6)	8.91 ± 0.36	2.31 ± 0.51**	ND	ND

See text for further details.
[a]Data are presented as the agonist $-\log EC_{50}$ in the presence of each treatment.
[b]Data are presented as the estimated half maximal voltage (in V) and frequency (in Hz) in the presence of each treatment. NB: 'Frequency + culture' represents experiments conducted in tissues after 3 days of organotypic culture.
*P < 0.05,**P < 0.01, ND, not determined.

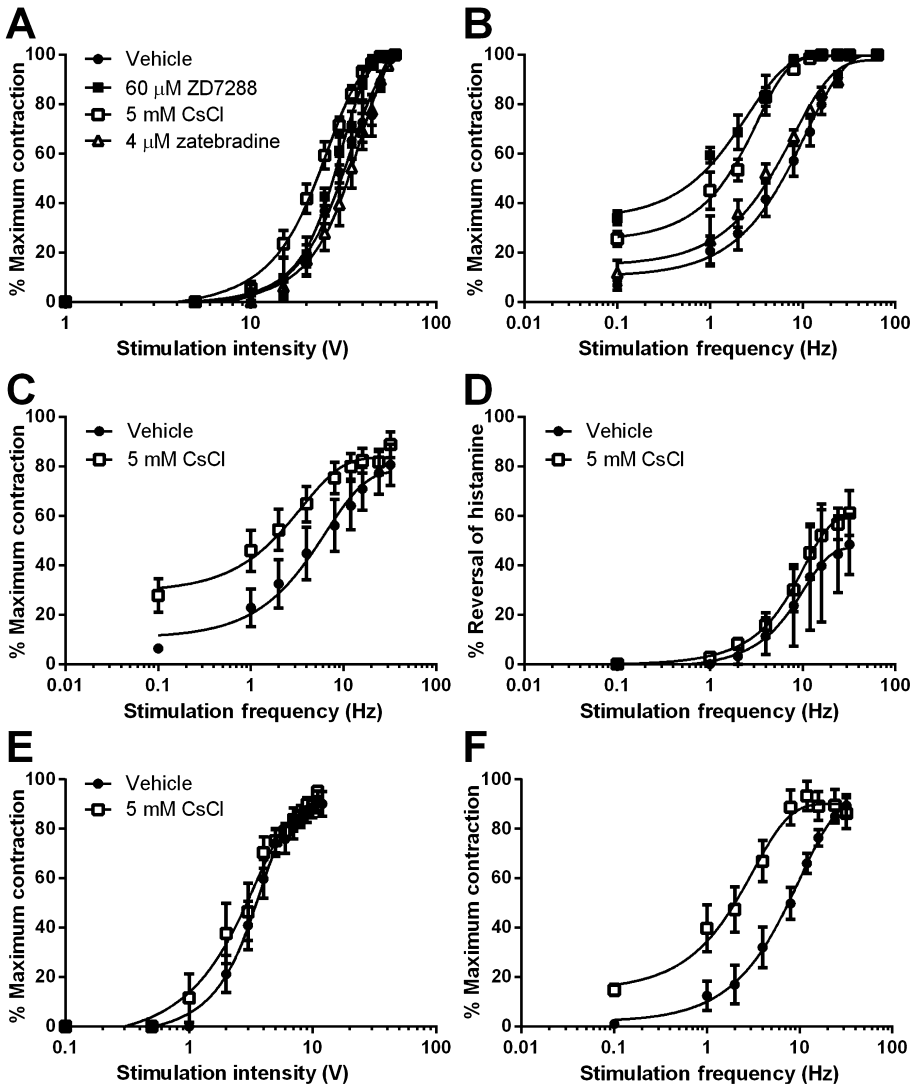

Figure 3

Effect of HCN channel inhibitors on parasympathetic-mediated control of airway smooth muscle tone *in vitro*. (A) Voltage- and (B) frequency-dependent EFS-evoked contractions of tracheal strips in the absence and presence of CsCl, ZD7288 or zatebradine. In (C) frequency-dependent EFS-evoked contractions were repeated in the absence or presence of CsCl in tissues that had been first maintained in organotypic culture for 3 days before the experiments. (D) Frequency-dependent EFS-evoked relaxations of tracheal strips in the absence or presence of CsCl. (E) Voltage- and (F) frequency-dependent vagus nerve stimulation-evoked contractions of innervated whole tracheal tube preparations in the absence or presence of CsCl. Each graph represents the mean ± SEM of four to six experiments. See also Table 1 and the text for additional details.

from the direct activation of postganglionic neurons, although preganglionic nerve terminals are also activated. In the presence of hexamethonium to negate any modulatory effects of preganglionic responses (and indomethacin, propranolol, CP99994, SR48968, SB220000 as described above), we compared voltage- and frequency-dependent contractions in the absence and presence of HCN channel inhibitors. Although Cs^+ produced a small (but statistically significant, $P < 0.05$) leftward shift in voltage-dependent contractions (at 32 Hz which is optimum for guinea pig tracheal contractions), this was not mimicked by ZD7288 or zatebradine (Figure 3A; Table 1). However, both Cs^+ and ZD7288 (but not zatebradine) markedly potentiated frequency-dependent responses (at the optimum stimulating intensity, determined for each tissue) (Figure 3B; Table 1). To confirm that the effects of the Cs^+ were due to an action on postganglionic neurons, we repeated the frequency-dependent contractions in tracheal tissues that had been maintained in an organotypic culture for 3 days before the EFS experiments. Under these conditions, the extrinsic neural innervation of the trachea degenerates (which includes parasympathetic preganglionic, sympathetic and sensory), whereas the intrinsic (parasympathetic postganglionic) innervation survives (see also Figure 6D). Organotypic culture failed to alter the potentiating effect of Cs^+, consistent with an action on postganglionic neurons (Figure 3C). Whereas parasympathetic

contractile responses were potentiated by HCN channel inhibitors, parasympathetic relaxant responses were largely unaffected (Figure 3D).

Consistent with the field stimulation experiments, activation of preganglionic nerve fibres via vagus nerve stimulation (in the absence of hexamethonium) in an innervated tracheal tube preparation produced voltage- and frequency-dependent contractions. Bath application of Cs^+ produced small effects on voltage-dependent contractions (particularly at lower stimulating voltages) but potentiated frequency responses to a magnitude comparable to EFS (Figure 3E and F; Table 1). To further assess preganglionic nerve-dependent responses we performed repeated short-train contractions of the innervated trachea by stimulating the vagi at a stimulus intensity evoking approximately 50% of the maximum contraction (10 s trains, 180 s inter-train intervals, for 80 min). In control tissues (no treatment), the magnitude of individual contractions was comparable across the duration of the experiment (Figure 4). Bath application of Cs^+ produced an initial transient (10 min) fall in contraction magnitude (21.6 ± 8.5% below baseline) followed by a reproducible and robust increase in contraction size which peaked at 122.8 ± 17.1% of the pretreatment maximum vagus-induced response ($P < 0.01$ significantly different from pretreatment control; Figure 4).

Unlike Cs^+, ZD7288 slowly inhibited preganglionic-evoked contractions under these conditions (Figure 4), producing a 26.3 ± 9.5% reduction in contraction magnitude by 60 min ($P < 0.05$, significantly lower than pretreatment control). This suggested that Cs^+ was acting via a mechanism that was not dependent on HCN channel inhibition. We therefore assessed a number of K^+ channel inhibitors to determine whether Cs^+ potentiates preganglionic nerve-dependent contractions via its ability to block a wide variety of K^+ channels. $BaCl_2$ at doses above 200 μM directly contracted the airway smooth muscle (not shown), making it difficult to study nerve-dependent responses. At 200 μM, $BaCl_2$ produced a small but significant ($P < 0.05$) increase in vagus nerve-dependent contractions (from 50.8 ± 2.57 to 63.9 ± 3.3% of the maximum vagus nerve-evoked response; Figure 4). TEA rapidly abolished all nerve-dependent contractions, whereas apamin (up to 1 μM) failed to produce any noticeable effect (Figure 4). The maxi-K^+ channel inhibitor iberiotoxin produced an increase in contraction magnitude that peaked at 40 min post-treatment (from 43.6 ± 6.4 to 78.7 ± 7.9% of the maximum vagus nerve-evoked response, $P < 0.05$; Figure 4). Increasing the concentration of iberiotoxin (from 100 nM to 1 μM) in one experiment did not further increase the magnitude of the potentiation. Finally 4-AP produced an immediate and sustained maximal contraction of the trachea, effectively abolishing vagus nerve-dependent responses (Figure 4). 4-AP-induced contractions were reduced approximately 50% by ganglionic blockade with hexamethonium, and entirely reversed by atropine (Figure 4).

Cs^+-evoked spontaneous preganglionic nerve activity

Cs^+ not only increased the magnitude of vagus nerve-evoked contractions in tracheal tube preparations, but with prolonged exposure increased basal resting tone and subsequently induced spontaneous bursting tracheal contractions, not dependent on electrical stimulation of the vagus nerves (Figure 5). The onset of the first autorhythmic contraction was 17.0 ± 4.9 min, and the average magnitude of these autorhythmic bursts after 60 min of recording was 29.6 ± 8.2% of the maximal tracheal contraction ($n = 8$), although individual peaks frequently exceeded the maximum vagus nerve-evoked responses (Figure 5). This effect was not mimicked by ZD7288, zatebradine or any of the potassium channel blocking compounds tested above, but was mimicked by 5 mM $CsCO_3$ (not shown). Cs^+-evoked autorhythmic contractions were completely silenced by atropine, which also restored resting tracheal tone (Figure 5A). Bath application of TTX also silenced Cs^+-evoked contractions, indicating that the response was nerve-dependent (Figure 5B). In experiments using EFS of tracheal tubes (rather than vagus nerve stimulation) Cs^+ similarly induced autorhythmicity, which was blocked entirely by bath application of hexamethonium (Figure 5C) leaving intact EFS (i.e. postganglionic)-induced responses. In these experiments, EFS-evoked contractions were predictably abolished by atropine. This suggested that prolonged Cs^+ exposure induces autorhythmic preganglionic nerve activity. To test this further we compared the effects of Cs^+ on control tissues (i.e. freshly harvested) versus tissues after organotypic culture for 3 days. Organotypic culture did not alter EFS-induced postganglionic nerve-dependent contractions (Figure 5D, left panels) but dramatically reduced the frequency of Cs^+-evoked autorhythmic contractions (Figure 5D, right panels).

Effect of ZD7288 on agonist-evoked contractions in vivo

In urethane-anaesthetized, mechanically ventilated guinea pigs i.v. injection of ZD7288 (2 mg·mL^{-1}) significantly ($P < 0.01$) lowered heart rate and mean arterial blood pressure (Figure 6A,B). In vehicle-treated animals, i.v. injection of capsaicin or histamine produced a dose-dependent increase in PIP, indicative of bronchoconstriction (Figure 6C,D). In ZD7288-treated animals, both capsaicin and histamine-evoked bronchoconstriction was significantly ($P < 0.05$) potentiated. Thus, the provocative dose causing 50% increase in PIP for capsaicin and histamine were 24.62 ± 3.99 and 5.95 ± 1.24 for vehicle versus 7.42 ± 0.73 and 0.96 ± 1.12 for ZD7288-treated animals respectively. Pretreatment of animals with the NK receptor antagonists CP99994 and SR48968 abolished capsaicin-evoked increases in PIP (Figure 6C). Blocking NK receptors was without effect on histamine-evoked bronchospasm in vehicle-treated animals (Figure 6D, dotted line), but reversed the potentiation of histamine-evoked bronchospasm in animals given ZD7288 (Figure 6D).

Expression of HCN channels

In guinea pig tissues, transcripts for all HCN channel subtypes were detected using RT-PCR in jugular ganglia and brainstem homogenates, whereas only HCN3 and HCN4 were found in the nodose ganglia (Figure 7). Trachealis muscle also expressed all four channel subtypes, whereas in the lung all but HCN2 were detected.

Immunohistochemical staining of rat tissues revealed that HCN2 and HCN4 were robustly expressed in many vagal

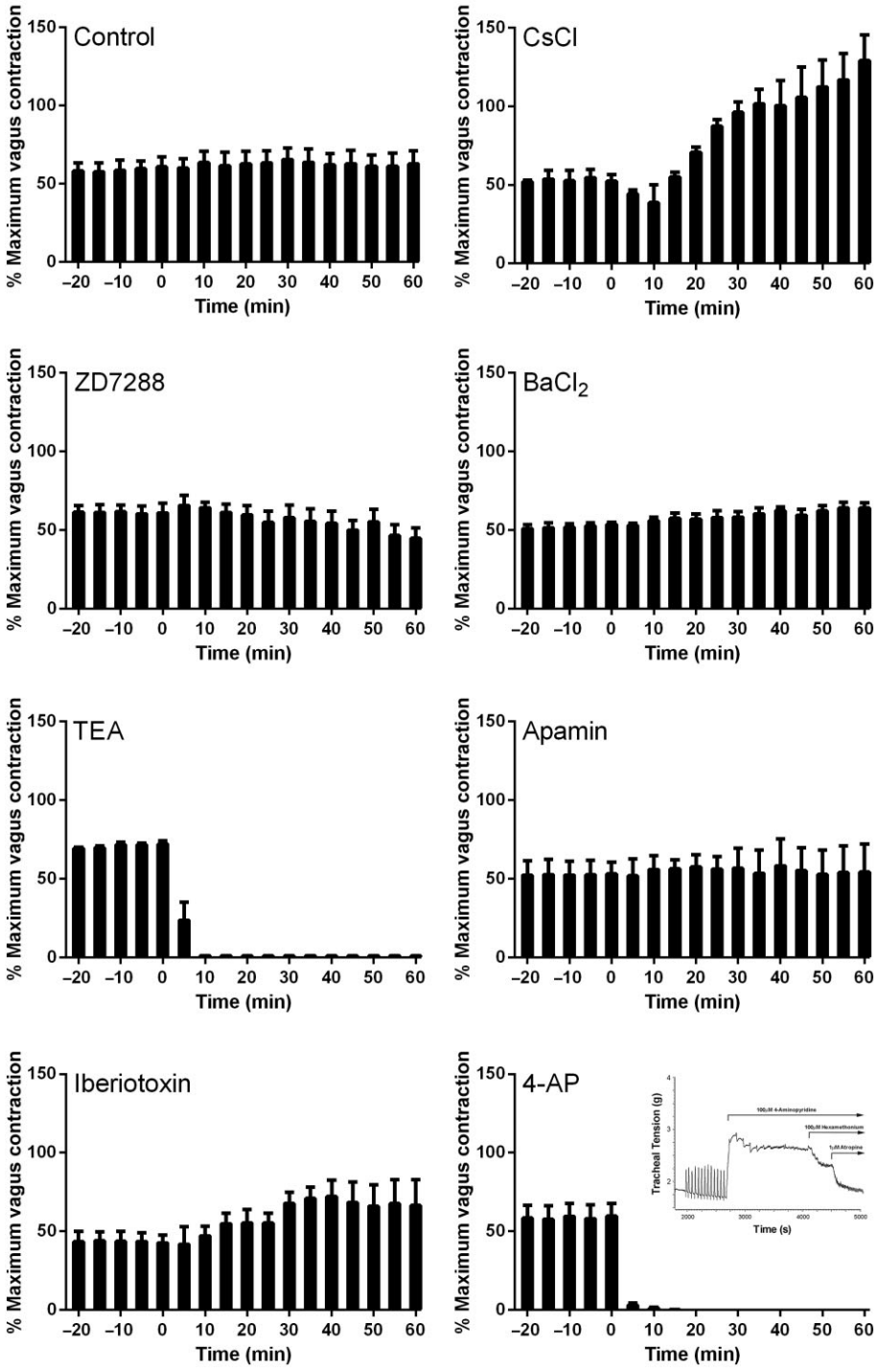

Figure 4

Effect of HCN channel and potassium channel inhibitors on repeated vagus nerve stimulation-evoked contractions of airway smooth muscle *in vitro*. Stable and reproducible subthreshold vagus nerve-dependent tracheal contractions were evoked over time (–20 to 0 min) before the addition (at time = 0) of vehicle (control), the HCN channel inhibitors (CsCl and ZD7288) or the potassium channel inhibitors (BaCl2, TEA, apamin, iberiotoxin and 4-AP). The magnitude of evoked contractions was measured for up to 60 min. Each graph represents the mean ± SEM of four to six experiments. *Inset*: representative trace showing the effect of 4-AP. Note that bath application of 4-AP produces a rapid near maximal contraction of the trachea, effectively inhibiting vagus nerve stimulation-evoked contractions, unlike TEA that inhibited contractions without altering baseline smooth muscle tone. The effect of 4-AP was reversed in part by bath application of hexamethonium and in whole by atropine, both of which also abolished vagus nerve-evoked responses.

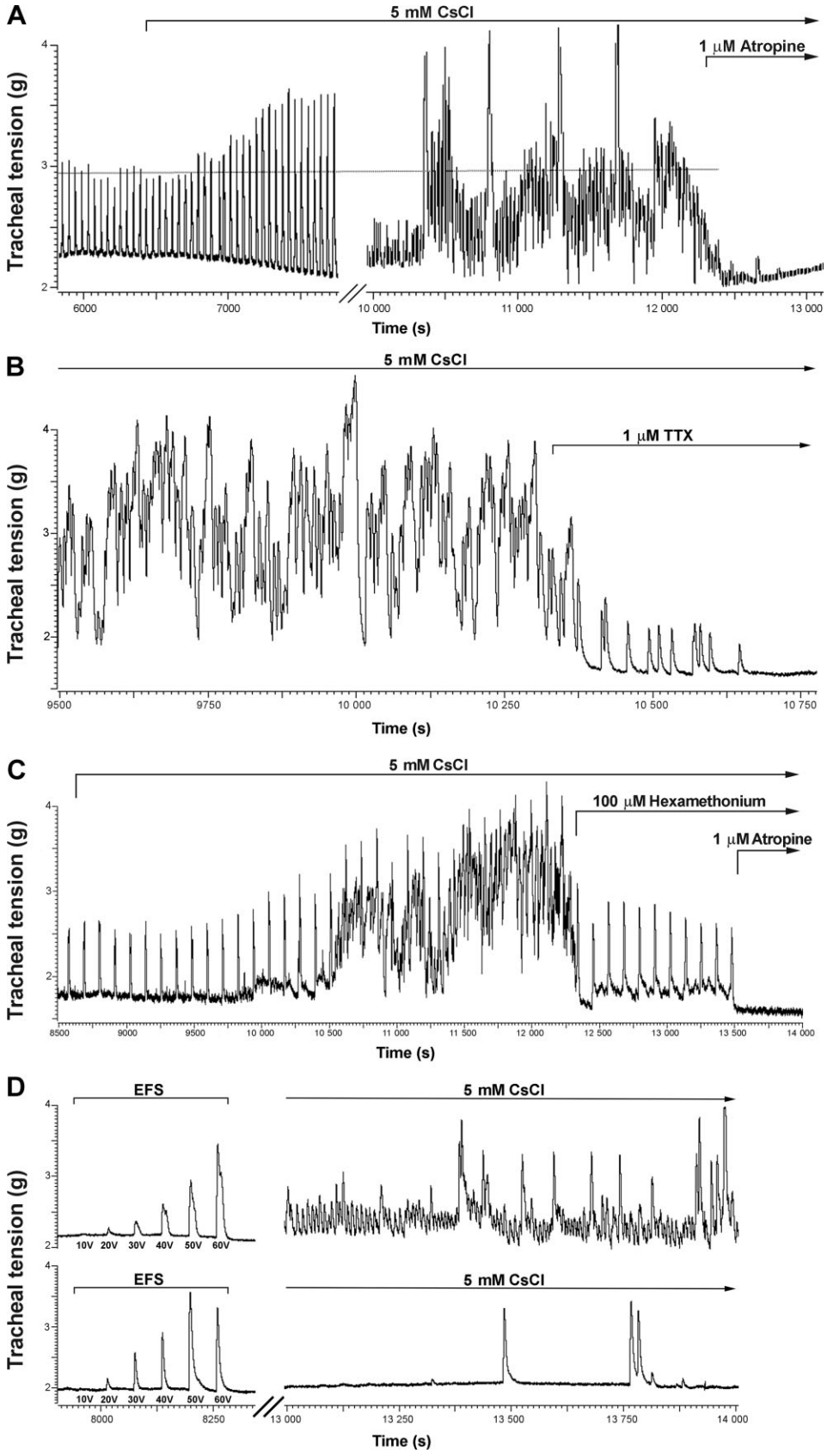
A
5 mM CsCl
1 μM Atropine
Tracheal tension (g)
Time (s)
B
5 mM CsCl
1 μM TTX
Tracheal tension (g)
Time (s)
C
5 mM CsCl
100 μM Hexamethonium
1 μM Atropine
Tracheal tension (g)
Time (s)
D
EFS
5 mM CsCl
10V 20V 30V 40V 50V 60V
EFS
5 mM CsCl
10V 20V 30V 40V 50V 60V
Tracheal tension (g)
Time (s)

Figure 5

Representative traces showing the effect of CsCl administered to innervated tracheal tube preparations *in vitro*. (A) Bath application of CsCl initially increases the magnitude of vagus nerve stimulation-evoked tracheal contractions (left panel, see also Figure 5 for mean data) and then subsequently induces spontaneous autorhythmic contractions independent of nerve stimulation (right panel). Both nerve stimulation and autorhythmic contractions are abolished by (A) atropine and (B) TTX. (C) EFS of tracheal tube preparations also evoked reproducible contractions that were potentiated by CsCl and converted to autorhythmic responses. Bath application of hexamethonium abolished the spontaneous autorhythmicity but preserved EFS-evoked contractions, whereas atropine abolished all responses. (D) The two representative traces show experiments conducted with freshly isolated tracheal tube preparations (upper trace) versus preparations after 3 days in organgotypic culture (lower trace). EFS produced comparable voltage-dependent responses in both preparations (indicative that postganglionic neurons were unaffected by organotypic culture), whereas CsCl-evoked spontaneous autorhythmicity was substantially reduced in tissues after culture. Each trace is representative of three to six similar experiments.

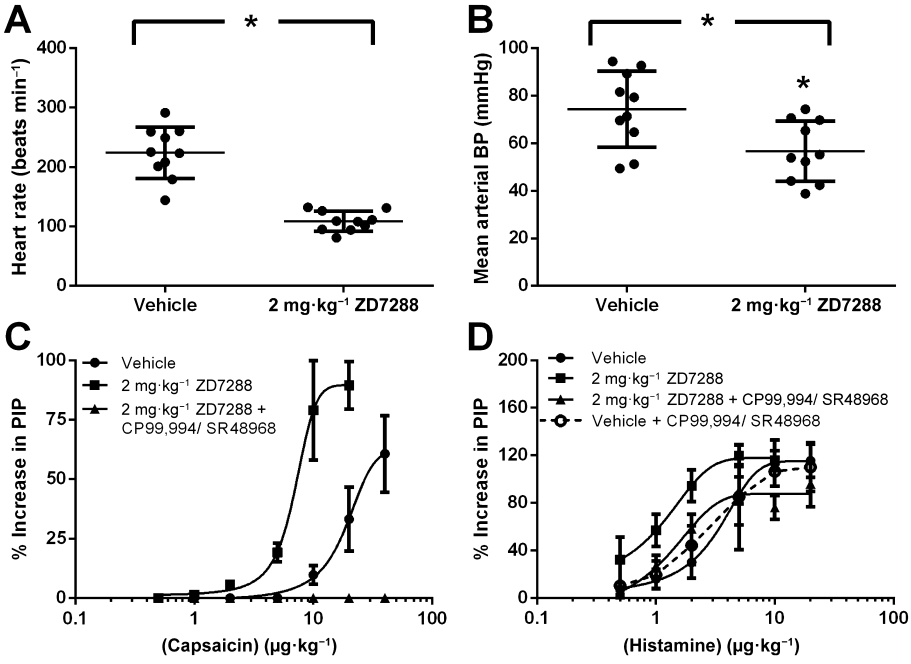

Figure 6

Effect of HCN channel inhibition on airway smooth muscle reactivity *in vivo*. In mechanically ventilated guinea pigs, i.v. pretreatment with ZD7288 (2 mg·kg^{-1}) significantly reduced (A) heart rate and (B) mean arterial blood pressure, relative to saline control (vehicle). ZD7288-potentiated bronchospasm (PIP) evoked by i.v. administered (C) capsaicin and (D) histamine. Before administration of the NK receptor antagonists CP99994 and SR48968 (0.3 mg·kg^{-1}) abolished all capsaicin-evoked bronchospasm. By contrast, the NK receptor antagonists had no effect on histamine-evoked bronchospasm in vehicle-treated animals (dashed line) but prevented the hyperresponsiveness induced by ZD7288. *$P < 0.01$, significantly different from vehicle control. Each graph represents the mean ± SEM of five experiments.

ganglia neurons, while HCN1 was present on the plasma membrane of a small subset of ganglia neurons (Figure 8A–C). For HCN2, staining was either on the cell membrane, cytoplasmic or purely nuclear in some cells, and although many nerve fibres within the ganglia were also HCN2-positive this was not true for HCN1 and HCN4 where no nerve fibre staining was evident. Consistent with this, HCN2-positive nerve fibre terminals were present in the brainstem nuclei in receipt of vagal afferent sensory projections (the spinal trigeminal nucleus and the nucleus of the solitary tract) and in the trachealis muscle (Figure 8E,F). No HCN channel staining (for any subtype) was observed in tracheal ganglia (airway post-ganglionic neurons) or the neurons of the rostral nucleus ambiguus (vagal preganglionic neurons) (McGovern and Mazzone, 2010); however, HCN1 staining was seen in laryngeal motor neurons in the caudal nucleus ambiguus (Figure 8D). HCN3 staining was not detected above background in rat ganglia, brainstem vagal nuclei or the airways. *In situ* hybridization performed on guinea pig vagal ganglia confirmed the expression of HCN1 and HCN2 in many jugular ganglia neurons, whereas HCN3 expression was detectable, but the staining intensity was not as robust as for HCN1 and HCN2 (Figure 8G–I). Detectable HCN4 staining was not found in the guinea pig jugular ganglia neurons, and only HCN3 was observed, albeit at very low expression levels, in the nodose ganglia (not shown).

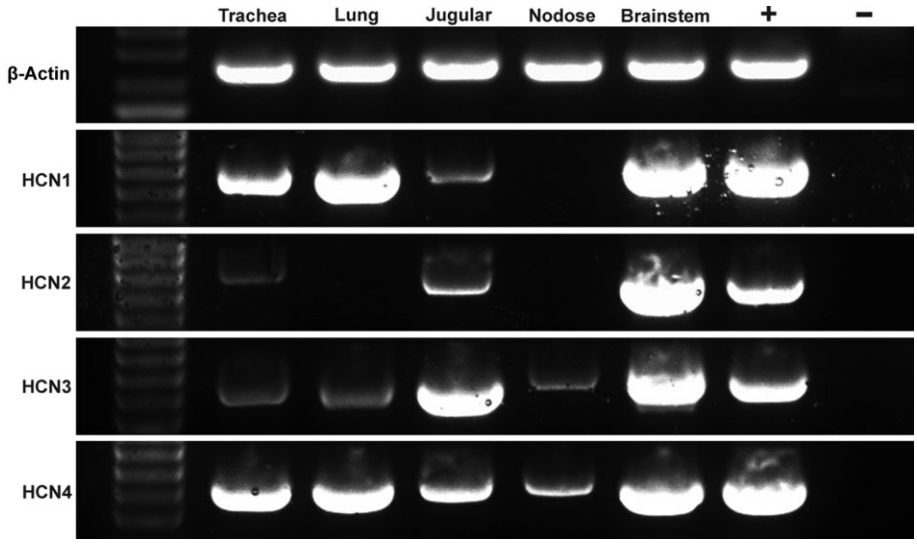

Figure 7
RT-PCR expression of HCN channel subtypes in guinea pig airway and neuronal tissues.

Discussion

Absence of HCN channel inhibitor effects on airway smooth muscle

HCN channel inhibitors have principally been developed to block the sinoatrial cardiac I_h current as a more selective means to induce bradycardia in patients with ischaemic and related heart diseases (Biel *et al.*, 2009). Indeed, one of the limitations of other cardio-inhibitory drugs, particularly non-selective β-adrenoceptor inhibitors (such as propranolol) is a profound direct effect on airway resistance due to antagonism of the airway smooth muscle relaxant effects of neurally released or circulating catecholamines, and it is thought that HCN channel inhibitors do not have direct effects in the airways. We detected PCR transcripts of all HCN channels in homogenates of airway tissues, suggesting that one or more cell types may be sensitive to HCN blockers. However, although smooth muscle cells in some organ systems may express hyperpolarization-activated currents that resemble I_h (e.g. Green *et al.*, 1996), there is limited evidence to suggest that airway smooth muscle cells express functional HCN channels and/or have any significant I_h current. For example, Snetkov *et al.* (1996) reported that approximately 20% of cultured smooth muscle cells isolated from third and fourth generation bronchi express a hyperpolarization-induced inwardly rectifying current, but this was absent in freshly isolated cells from the same airway level suggesting that it emerged as an artefact of the cell culture conditions. Our data support an absence of functional HCN channel-dependent responses in airway smooth muscle, which did not contract directly to concentrations of ZD7288 or Cs^+ that are selective for HCN channel blockade (although Cs^+ did contract the airway smooth muscle at higher concentrations, presumably unrelated to HCN channels). ZD7288 and Cs^+ also had no effect on smooth muscle contractions evoked by several bronchospastic agonists. However, airway smooth muscle cells are not homogeneous and the absence or presence of an HCN channel-mediated current may be dependent on the size of the airways from which smooth muscle cells are studied. Thus, freshly isolated cells from small intralobar bronchioles express a Cs^+-sensitive hyperpolarization-induced current (Snetkov and Ward, 1999). Our studies (including our *in vivo* experiments, see below) measured responses of large airways, and therefore we cannot rule out the possibility that smaller airways may behave differently in response to HCN channel inhibition.

Although HCN channel inhibition *per se* did not directly alter airway smooth muscle tone, the HCN channel inhibitor zatebradine was a relatively potent constrictor of tracheal smooth muscle. Zatebradine-induced bronchospasm occurred at doses (1–10 μM) well within the reported EC_{50} for HCN channel inhibition (which is approximately 2 μM at cloned HCN channels; Stieber *et al.*, 2006) but was not mimicked by ZD7288 or Cs^+ at concentrations reportedly selective for HCN channels (Marshall *et al.*, 1993; Doan *et al.*, 2004; Stieber *et al.*, 2005), suggesting that it was unrelated to an action at HCN channels. Zatebradine contractions were not altered by inhibitors of neurally-evoked responses (atropine and NK receptor antagonists), but was abolished by blocking histamine H_1 receptors. We are not aware of any previously published reports specifically showing a histaminergic action of zatebradine, although this is alluded to in a study by Maesen *et al.* (1994) who cite unpublished work, and also show that zatebradine leads to deterioration in pulmonary function in asthmatic patients.

HCN channel inhibitors regulate airway sensory nerve excitability

Subsets of visceral and somatic sensory neurons express functional HCN channels. In the vagal sensory ganglia (where the majority of airway afferent nerves originate), immunohistochemical staining has shown sensory soma to express HCN1, HCN2 and HCN4 (in rats) or HCN2 and HCN3 (in mice), and

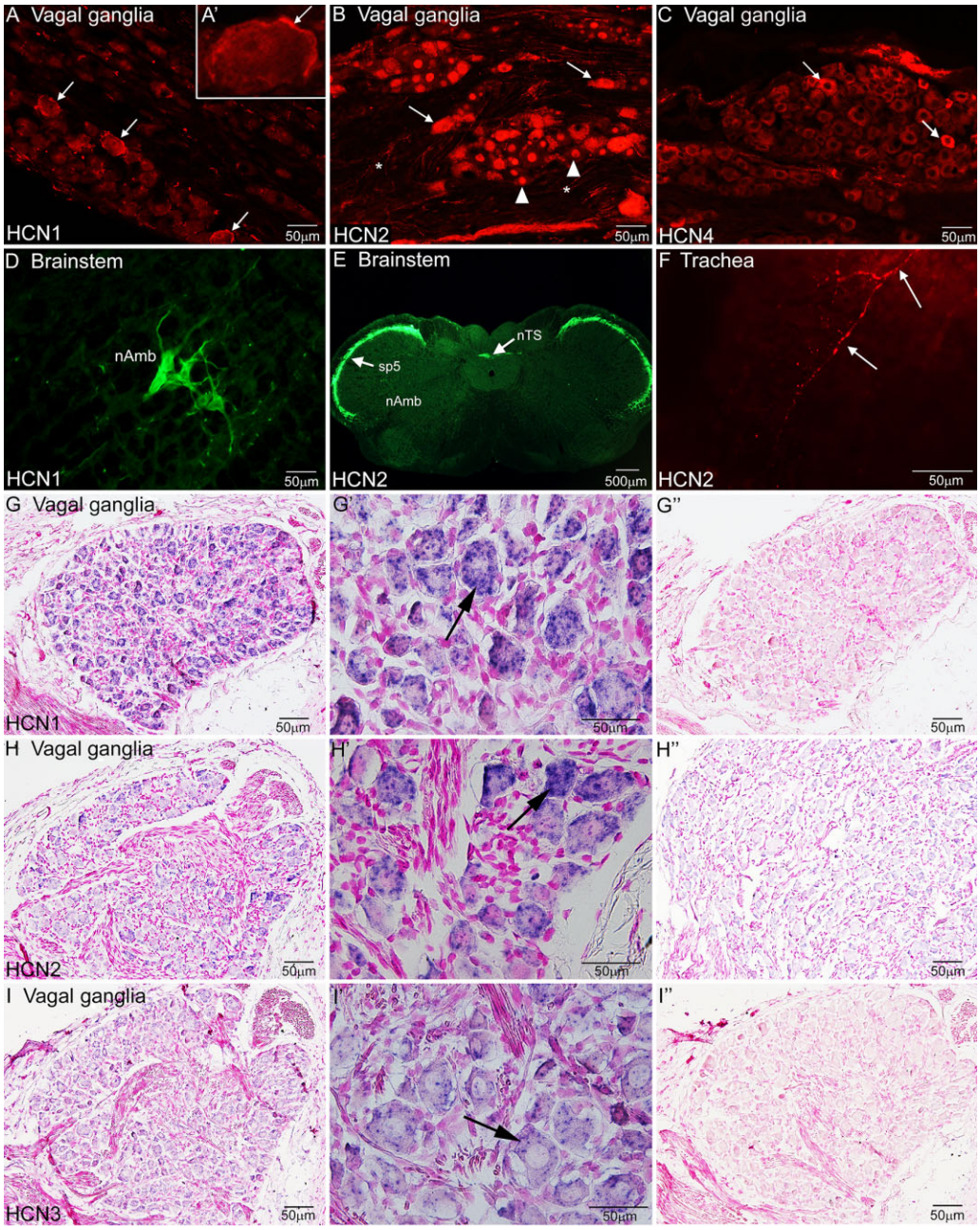

Figure 8

Expression of HCN channel subtypes in neuronal tissues innervating the airways. (A–F) Immunohistochemical staining in rat vagal ganglia (A–C), brainstem (D,E) and trachea (F). (G–I) *In situ* hybridization staining in guinea pig jugular ganglia. (A') A high magnification of a neuron with plasma membrane staining for HCN1. In (A–C), arrows show examples of positively labelled neurons. In (B) staining in some neurons was purely nuclear (arrow heads). HCN2 expressing nerve fibres are also seen in the ganglia (asterisks). (G and G', H and H', I and I') Antisense riboprobe staining of guinea pig jugular ganglia at low and high magnification. Arrows show examples of stained neurons. (G", H", I") Negative (sense riboprobe) controls. nAmb, nucleus ambiguus; nTS, nucleus of the solitary tract; sp5, spinal trigeminal tract.

mRNA transcripts for all HCN channel subtypes can be detected in rat vagal ganglia (Doan *et al.*, 2004; Wang *et al.*, 2012). In our immunohistochemical studies using rat vagal ganglia sections, we observed HCN1, HCN2 and/or HCN4 staining in subsets of neurons and/or nerve fibres. Consistent with this, we detected PCR transcripts for all four HCN channels in homogenates of guinea pig jugular ganglia, HCN3 and HCN4 in homogenates of guinea pig nodose ganglia, and with *in situ* hybridization we noted neuronal expression of HCN1, HCN2 and HCN3 in tissue sections of guinea pig vagal ganglia. Electrophysiological studies of isolated vagal ganglia neurons confirm the presence of I_h in many vagal ganglia neurons (Undem and Weinreich, 1993; Ingram and Williams, 1996; Doan *et al.*, 2004; Wang *et al.*, 2012). With respect to

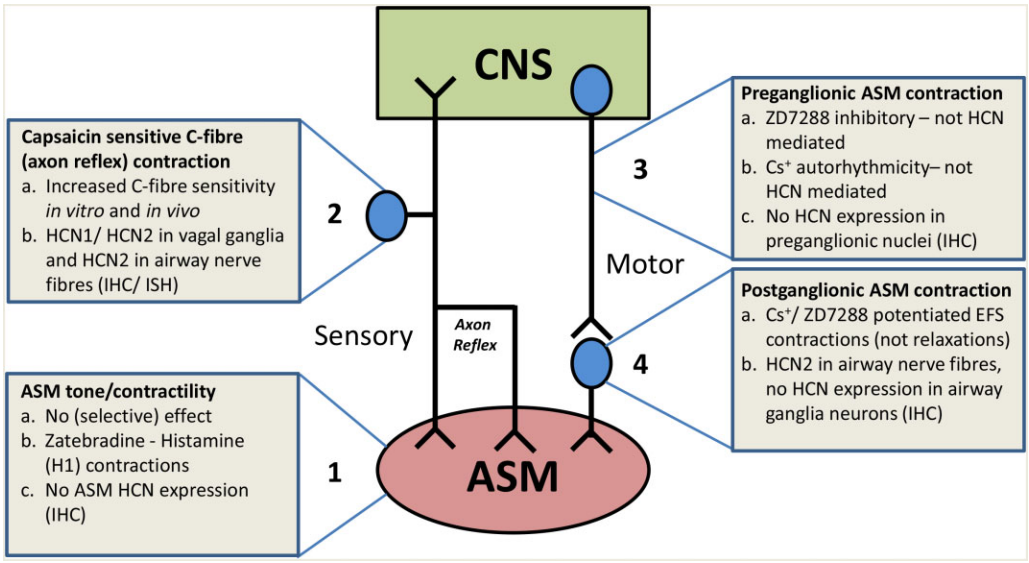

Figure 9

Schematic diagram showing the organization of the neural innervation to the airways and the major outcomes of the study. The airway smooth muscle (ASM) is innervated by both sensory and motor neural pathways that can regulate ASM tone by peptidergic (sensory axon reflex) and cholinergic (contractile motor)/non-cholinergic (relaxant motor) neurotransmitters. The present study assessed the effect of HCN channel inhibitors on (i) the airway smooth muscle directly; (ii) sensory-mediated contractions; (iii) preganglionic driven contractions; and (iv) postganglionic contractions and relaxations.

guinea pig, up to 30% of nodose (inferior vagal ganglia) neurons have a Cs^+-sensitive inwardly rectifying current in response to membrane hyperpolarizations (Undem and Weinreich, 1993) and these currents are modulated by cAMP and related analogues (Ingram and Williams, 1996) consistent with the expression of HCN channels.

The functional and expression data clearly suggest that HCN channel expression is not homogeneous across all subsets of vagal sensory neurons. Rather, important differences probably exist between A-fibre and C-fibre sensory neurons in both the channel subtype expressed and its sensitivity to cyclic nucleotides. As a consequence, the functional significance of HCN channels in vagal sensory neurons is at present unclear. For example, blockade of I_h with Cs^+ leads to hyperpolarization of the resting membrane potential in mechanosensitive nodose neurons innervating the aortic arch (i.e. baroreceptor neurons), and this is associated with a substantial increase in membrane input resistance and as a consequence the threshold of stretch-induced baroreceptor discharge is reduced (Doan *et al.*, 2004). This is seemingly consistent with our data showing that both Cs^+ and/or ZD7288 (both *in vitro* and *in vivo*) significantly increase airway reactivity to capsaicin (Figure 9), a compound that evokes airway smooth muscle constriction secondary to activating capsaicin-sensitive NK-expressing vagal afferent nerves (which are uniformly C-fibres in the guinea pig airways). In stark contrast, blocking I_h with either Cs^+ or ZD7288 reduces the excitability of isolated A-type fibre vagal afferent neurons, and reduces spontaneous afferent firing in models of neuropathic pain (Jiang *et al.*, 2008; Zhou *et al.*, 2010). These opposing observations suggest that HCN channels probably play complex roles in regulating sensory neuron excitability beyond that of simply setting resting membrane potential through I_h. Indeed, modelling experiments using the properties of hippocampal neurons have suggested that interactions between HCN and other channels (e.g. TASK-like K^+ channels) might explain some of these anomalies in excitability (Migliore and Migliore, 2012).

Of interest in the present study was the effect of i.v. administered ZD7288 on the bronchoconstriction evoked by subsequent i.v. administration of histamine. Histamine induces contraction of airway smooth muscle that is principally mediated by H_1 receptors expressed on the smooth muscle cells, but also partially dependent on the bronchospasm activating mechanosensitive (A-fibre) airway afferents, which then reflexively increase parasympathetic cholinergic output to the airway smooth muscle (Canning *et al.*, 2001). When evaluating PIP, the cholinergic component of the response to i.v. histamine is not readily differentiated from the direct effects of histamine on the smooth muscle because of the nature of PIP recordings. Regardless, histamine does not induce firing in airway vagal C-fibres and, therefore, histamine-induced obstruction does not have a NK-dependent component (Undem and Weinreich, 1993; Canning *et al.*, 2001). This is consistent with our control experiments in the presence of NK receptor antagonists. However, i.v. pretreatment of animals with ZD7288 unmasked a NK-dependent component to the histamine-evoked bronchospasm, which served to increase reactivity to histamine. This suggests that in the presence of HCN channel blockade, airway C-fibres can be activated by i.v. histamine and this again supports the suggestion that HCN channel inhibition increases the excitability of C-fibres in the airways. Given that tachykinergic sensory neurons innervating the guinea pig airways are largely derived from the jugular ganglia (Nassenstein *et al.*, 2010) and HCN2 was

detected by immunohistochemistry in vagal subsets of ganglia neurons, as well as in airway nerve fibres, it seems likely that HCN2 contributes at least in part to the functional effects of HCN channel inhibitors on C-fibres noted in the present study.

HCN channel inhibitors regulate airway parasympathetic nerve excitability

The efferent neural control of airway smooth muscle tone is principally derived from vagal parasympathetic pathways. Thus, parasympathetic contractile (cholinergic) and relaxant (noncholinergic) postganglionic neurons are regulated by vagal preganglionic neurons that originate in brainstem vagal motor nuclei (McGovern and Mazzone, 2010). Guinea pigs have a functional sympathetic input to the airway smooth muscle (Oh *et al.*, 2006), but this is not representative of the human airways that lack any direct significant sympathetic neural control over airway smooth muscle tone (Richardson and Béland, 1976). For these reasons, we confined the experiments in the present study to vagal pathways only. With respect to HCN channels, neurons in the compact regions of the nucleus ambiguus, where airway preganglionic neurons originate (McGovern and Mazzone, 2010), have demonstrable I_h currents (Nishimura *et al.*, 1995). However, the specific channel mediating I_h in ambiguus neurons has not been reported. In the present study, all HCN channels were detected with RT-PCR in brainstem homogenates; however, no HCN channel expression was detected in vagal preganglionic neurons within the rostral nucleus ambiguus with immunohistochemistry. In the caudal nucleus ambiguus, laryngeal motor neurons stained intensely for HCN1, consistent with previous reports (Milligan *et al.*, 2006). There have been no previous studies assessing whether airway postganglionic neurons have I_h, although neurons in other autonomic ganglia (e.g. cardiac, celiac and vestibular ganglia) have been shown to express functional HCN channels (Vanner *et al.*, 1993; Lamas, 1998; Tompkins *et al.*, 2009). Indeed, we found all HCN transcripts by PCR at different levels of the tracheobronchial tree, but failed to see any HCN channel expression with immunohistochemistry airway ganglia. Immunohistochemically stained nerve fibres were present in tracheal wholemounts, but whether these represent postganglionic nerve fibres or the peripheral terminals of vagal afferent neurons is unclear at present.

The results of our studies suggest heterogeneous effects of HCN channel inhibitors on parasympathetic neurons regulating airway smooth muscle tone (Figure 9). Cs^+ and ZD7288 potentiated field stimulation-evoked contractions, which under the experimental conditions employed (i.e. in the presence of hexamethonium to block preganglionic transmission and NK receptor antagonists to inhibit C-fibre responses) reflect an increased responsiveness of postganglionic neurons. This was confirmed using organotypic culture to remove preganglionic terminals from the airways. However, the effect of HCN channel inhibitors was not on the electrical excitability of the evoked responses, as the voltage-dependency of field stimulation-evoked responses was largely unchanged, but rather on the magnitude of contraction per stimulus pulse. This might suggest that HCN channel inhibition increases the quanta of neurotransmitter released per action potential from airway postganglionic neurons. Similar responses have been reported in neocortical slices where ZD7288 potentiates transmitter release from noradrenergic neurons (Klar *et al.*, 2003). By stark contrast, blocking HCN channels produced no significant effect on non-cholinergic postganglionic relaxant responses in the guinea pig airways, perhaps suggesting that this subset of postganglionic neurons, which uniquely originate in the myenteric plexus of the adjacent oesophagus (Fischer *et al.*, 1998), may not be sensitive to HCN channel inhibition. The mechanism by which postganglionic potentiation occurred is unclear, given that we did not find HCN channel expression in airway ganglia. It may be that the effect on postganglionic neurons is mediated by the altered excitability of airway C-fibres, which are known to modulate ganglionic transmission via tachykinergic mechanisms (Canning *et al.*, 2002). However, such a mechanism in our study would need to be independent of tachykinins, as all experiments included tachykinin receptor antagonists at concentrations sufficient to abolish tachykinin-mediated responses.

When preganglionic nerve fibres were directly stimulated via vagus nerve stimulation, Cs^+ similarly potentiated frequency-dependent responses. However, the magnitude of this potentiation was comparable with that observed with field stimulation in the presence of hexamethonium, suggesting that HCN channel inhibitors potentiate frequency-dependent vagal responses predominately due to an effect on postganglionic neurons. At half maximal voltages, with a supramaximal frequency to prevent any potential change in postganglionic nerve frequency dependency, ZD7288 slowly inhibited preganglionic-evoked contractions. This was not the case in the same experiments employing Cs^+, in which preganglionic-evoked tracheal contractions were increased in magnitude. Furthermore, in the continued presence of Cs^+ stimulus-independent tracheal contractions emerged that were due to an induction of spontaneous activity in preganglionic fibres innervating the airways (in as much as the contractions were inhibited by either TTX or hexamethonium). It is at present unclear as to the mechanism by which Cs^+ induced this preganglionic activity, but this effect was not mimicked by a number of common K^+ channel inhibitors, including compounds that block both outwardly and inwardly rectifying K^+ conductances as well as Ca^{2+} activated small and large conductance potassium channels. A similar bursting response has been reported in electrophysiological studies of sympathetic preganglionic neurons in the spinal cord following intracellular Cs^+ loading (Wilson *et al.*, 2002). In these studies, replacing intracellular potassium with equimolar concentrations of Cs^+ (140 mM) to block all K^+ conductances revealed a low threshold Ca^{2+} conductance, presumably mediated by T-type Ca^{2+} channels, which mediated burst firing and autorhythmicity. Whether bath application of 5 mM Cs^+ in our experiments is capable of accumulating intracellularly in airway vagal preganglionic axons, to a level sufficient to block K^+ conductances and unmask a low threshold Ca^{2+} conductance, is unknown, but some K^+ channels are permeable to Cs^+ and this might provide a mechanism for intracellular accumulation. Although we have noted in preliminary experiments ($n = 3$) that the T-type Ca^{2+} channel blocker NNC 55-0396 fails to inhibit Cs^+-evoked preganglionic autorhythmicity

(*unpublished observations*), which is inconsistent with this hypothesis.

Methodological considerations

The preparations employed in this study have been well validated to study nerve-mediated responses in the airways. However, as with all pharmacological studies it is important to consider aspects of the selectivity of the compounds under study. Zatebradine has a reported EC_{50} of 2 μM at HCN channels, without displaying any subtype specificity (Stieber *et al.*, 2006). However, we noted that at concentrations as low as 1 μM zatebradine showed agonist activity at histamine H_1 receptors and, therefore, chose to limit our experiments with this compound. ZD7288 is perhaps the best-studied HCN channel inhibitor. It is acting on the intracellular side of HCN channels and has a reported EC_{50} of 20–40 μM at each of the four HCN channel subtypes, although when applied extracellularly in tissue preparations it is often used at concentrations of up to 100 μM as it does not easily cross the cell membrane (Stieber *et al.*, 2005). ZD7288 can have several off-target effects, including blocking inward Na^+ currents in dorsal root ganglia neurons with an EC_{50} of close to 10 μM (Wu *et al.*, 2012) and T-type Ca^{2+} channels with an EC_{50} of 100 μM (Felix *et al.*, 2003). Blockade of Na^+ channels would be expected to inhibit the nerve-evoked responses under investigation in the present study, and may perhaps explain the effect of ZD7288 on preganglionic-evoked contractions that were inhibited. Inhibition of T-type Ca^{2+} channels (with Ni^+) potentiates cholinergic nerve-dependent airway contractions at low and high stimulating frequencies (Shih *et al.*, 2010), somewhat consistent with the effect of ZD7288 (and Cs^+) on postganglionic responses in the present study. Cs^+ acts at low mM concentrations to block I_h (DiFrancesco, 1982) and is well known as a non-specific K^+ channel inhibitor blocking Ba^{2+} sensitive inwardly rectifying K^+ channels in the mM range and others at higher concentrations. However, we are unaware of any data showing that Cs^+ can block T-type Ca^{2+} currents, which might argue against a role for T-type Ca^{2+} channels in the potentiation of cholinergic and C-fibre evoked responses produced by both ZD7288 and Cs^+ in the present study.

Summary and conclusions

Pharmacological inhibition of I_h (e.g. with ivabradine) is an established therapy for patients with cardiac arrhythmias or ischaemic heart disease. Recent studies have also suggested that HCN channel inhibitors may be useful in a number of nervous system diseases, including epilepsy and neuropathic pain (reviewed in Emery *et al.*, 2012; Shah *et al.*, 2013). However, there have been no previous studies exploring the effect of HCN channel inhibitors on the control of airway smooth muscle tone. Our data suggest that HCN channel inhibition has negligible direct effects on airway smooth muscle, although zatebradine may have off-target bronchospastic effects mediated by an action at histamine receptors. At doses selective for HCN channel inhibition, both Cs^+ and ZD7288 significantly potentiated nociceptive sensory- and parasympathetic postganglionic-mediated bronchospasm, consistent with the expression of HCN2 in airway nerve fibres. By contrast, the HCN channel inhibitor ZD7288 inhibited preganglionic nerve-mediated changes in airway smooth muscle tone *in vitro*, whereas Cs^+ potentiated preganglionic nerve-evoked responses and evoked spontaneous activity in vagal preganglionic neurons, but both effects are probably unrelated to HCN channel inhibition. ZD7288 administered *in vivo* increased airway reactivity and this is likely to be due to its sensitizing effect on pulmonary C-fibre nociceptors. Taken together the data suggest that HCN channel inhibitors have important effects on resting and neurally-evoked changes in airway smooth muscle tone, which have not been previously recognized. This finding may have implications for some patients receiving HCN channel inhibitors for therapeutic purposes.

Acknowledgements

This work was funded by grants to S. B. M. from the National Health and Medical Research Council (NH&MRC) of Australia (350333, 1025589, 1042528).

Conflict of interest

None.

References

Alexander SPH, Benson HE, Faccenda E, Pawson AJ, Sharman JL, Spedding M, Peters JA, Harmar AJ and CGTP Collaborators (2013). The Concise Guide to PHARMACOLOGY 2013/14: Ion channels. Br J Pharmacol 170: 1607–1651.

Belvisi MG, Stretton CD, Yacoub M, Barnes PJ (1992). Nitric oxide is the endogenous neurotransmitter of bronchodilator nerves in humans. Eur J Pharmacol 210: 221–222.

Biel M, Wahl-Schott C, Michalakis S, Zong X (2009). Hyperpolarization-activated cation channels: from genes to function. Physiol Rev 89: 847–885.

Canning BJ (2006). Reflex regulation of airway smooth muscle tone. J Appl Physiol 101: 971–985.

Canning BJ, Undem BJ (1993). Evidence that distinct neural pathways mediate parasympathetic contractions and relaxations of guinea-pig trachealis. J Physiol 471: 25–40.

Canning BJ, Reynolds SM, Mazzone SB (2001). Multiple mechanisms of reflex bronchospasm in guinea pigs. J Appl Physiol 91: 2642–2653.

Canning BJ, Reynolds SM, Anukwu LU, Kajekar R, Myers AC (2002). Endogenous neurokinins facilitate synaptic transmission in guinea pig airway parasympathetic ganglia. Am J Physiol Regul Integr Comp Physiol 283: R320–R330.

DiFrancesco D (1982). Block and activation of the pace-maker channel in calf purkinje fibres: effects of potassium, caesium and rubidium. J Physiol 329: 485–507.

Doan TN, Stephans K, Ramirez AN, Glazebrook PA, Andresen MC, Kunze DL (2004). Differential distribution and function of hyperpolarization-activated channels in sensory neurons and mechanosensitive fibers. J Neurosci 24: 3335–3343.

Emery EC, Young GT, McNaughton PA (2012). HCN2 ion channels: an emerging role as the pacemakers of pain. Trends Pharmacol Sci 33: 456–463.

Felix R, Sandoval A, Sánchez D, Gómora JC, De la Vega-Beltrán JL, Treviño CL *et al*. (2003). ZD7288 inhibits low-threshold Ca(2+) channel activity and regulates sperm function. Biochem Biophys Res Commun 311: 187–192.

Fischer A, Canning BJ, Undem BJ, Kummer W (1998). Evidence for an esophageal origin of VIP-IR and NO synthase-IR nerves innervating the guinea pig trachealis: a retrograde neuronal tracing and immunohistochemical analysis. J Comp Neurol 394: 326–334.

Green ME, Edwards G, Kirkup AJ, Miller M, Weston AH (1996). Pharmacological characterization of the inwardly-rectifying current in the smooth muscle cells of the rat bladder. Br J Pharmacol 119: 1509–1518.

Ingram SL, Williams JT (1996). Modulation of the hyperpolarization-activated current (Ih) by cyclic nucleotides in guinea-pig primary afferent neurons. J Physiol 492 (Pt 1): 97–106.

Jiang YQ, Xing GG, Wang SL, Tu HY, Chi YN, Li J *et al*. (2008). Axonal accumulation of hyperpolarization-activated cyclic nucleotide-gated cation channels contributes to mechanical allodynia after peripheral nerve injury in rat. Pain 37: 495–506.

Kilkenny C, Browne W, Cuthill IC, Emerson M, Altman DG (2010). Animal research: reporting *in vivo* experiments: the ARRIVE guidelines. Br J Pharmacol 160: 1577–1579.

Klar M, Surges R, Feuerstein TJ (2003). Ih channels as modulators of presynaptic terminal function: ZD7288 increases NMDA-evoked [3H]-noradrenaline release in rat neocortex slices. Naunyn Schmiedebergs Arch Pharmacol 367: 422–425.

Lamas JA (1998). A hyperpolarization-activated cation current (Ih) contributes to resting membrane potential in rat superior cervical sympathetic neurones. Pflugers Arch 436: 429–435.

Liu J, Zhang L, Tu H, Li YL (2012). Angiotensin II induces protein overexpression of hyperpolarization-activated cyclic nucleotide-gated channels in primary cultured nodose neurons. Neurosci Lett 515: 168–173.

Maesen FP, Smeets JJ, van Noord JA, Nehmiz G, Wald FD, Cornelissen PJ (1994). Effect of zatebradine, a novel 'sinus node inhibitor', on pulmonary function compared to placebo. Pulm Pharmacol 7: 349–355.

Marshall PW, Rouse W, Briggs I, Hargreaves RB, Mills SD, McLoughlin BJ (1993). ICI D7288, a novel sinoatrial node modulator. J Cardiovasc Pharmacol 21: 902–906.

Mazzone SB, Canning BJ (2002a). Synergistic interactions between airway afferent nerve subtypes mediating reflex bronchospasm in guinea pigs. Am J Physiol Regul Integr Comp Physiol 283: R86–R98.

Mazzone SB, Canning BJ (2002b). An in vivo guinea pig preparation for studying the autonomic regulation of airway smooth muscle tone. Auton Neurosci 99: 91–101.

Mazzone SB, Canning BJ (2002c). Evidence for differential reflex regulation of cholinergic and noncholinergic parasympathetic nerves innervating the airways. Am J Respir Crit Care Med 165: 1076–1083.

Mazzone SB, McGovern AE (2010). Innervation of tracheal parasympathetic ganglia by esophageal cholinergic neurons: evidence from anatomic and functional studies in guinea pigs. Am J Physiol Lung Cell Mol Physiol 298: L404–L416.

McGovern AE, Mazzone SB (2010). Characterization of the vagal motor neurons projecting to the Guinea pig airways and esophagus. Front Neurol 1: 153.

McGrath J, Drummond G, McLachlan E, Kilkenny C, Wainwright C (2010). Guidelines for reporting experiments involving animals: the ARRIVE guidelines. Br J Pharmacol 160: 1573–1576.

Migliore M, Migliore R (2012). Know your current I(h): interaction with a shunting current explains the puzzling effects of its pharmacological or pathological modulations. PLoS ONE 7: e36867.

Milligan CJ, Edwards IJ, Deuchars J (2006). HCN1 ion channel immunoreactivity in spinal cord and medulla oblongata. Brain Res 1081: 79–91.

Myers AC, Undem BJ (1991). Analysis of preganglionic nerve evoked cholinergic contractions of the guinea pig bronchus. J Auton Nerv Syst 35: 175–184.

Myers AC, Undem BJ (1993). Electrophysiological effects of tachykinins and capsaicin on guinea-pig bronchial parasympathetic ganglion neurones. J Physiol 470: 665–679.

Myers AC, Undem BJ, Weinreich D (1990). Electrophysiological properties of neurons in guinea pig bronchial parasympathetic ganglia. Am J Physiol 259 (6 Pt 1): L403–L409.

Myers AC, Undem BJ, Weinreich D (1991). Influence of antigen on membrane properties of guinea pig bronchial ganglion neurons. J Appl Physiol 71: 970–976.

Nassenstein C, Taylor-Clark TE, Myers AC, Ru F, Nandigama R, Bettner W *et al*. (2010). Phenotypic distinctions between neural crest and placodal derived vagal C-fibres in mouse lungs. J Physiol 588 (Pt 23): 4769–4783.

Nishimura Y, Muramatsu M, Asahara T, Tanaka T, Yamamoto T (1995). Electrophysiological properties and their modulation by norepinephrine in the ambiguus neurons of the guinea pig. Brain Res 702: 213–222.

Nof E, Antzelevitch C, Glikson M (2010). The contribution of HCN4 to normal sinus node function in humans and animal models. Pacing Clin Electrophysiol 33: 100–106.

Oh EJ, Mazzone SB, Canning BJ, Weinreich D (2006). Reflex regulation of airway sympathetic nerves in guinea-pigs. J Physiol 573 (Pt 2): 549–564.

Richardson J, Béland J (1976). Nonadrenergic inhibitory nervous system in human airways. J Appl Physiol 41 (5 Pt 1): 764–771.

Shah MM, Huang Z, Martinello K (2013). HCN and KV7 (M-) channels as targets for epilepsy treatment. Neuropharmacology 69: 75–81.

Shih CH, Hsu HT, Wang KH, Shih CH, Ko WC (2010). Calcium channel subtypes for cholinergic and nonadrenergic noncholinergic neurotransmission in isolated guinea pig trachea. Naunyn Schmiedebergs Arch Pharmacol 382: 419–432.

Simmons DG, Natale DR, Begay V, Hughes M, Leutz A, Cross JC (2008). Early patterning of the chorion leads to the trilaminar trophoblast cell structure in the placental labyrinth. Development 135: 2083–2091.

Snetkov VA, Ward JP (1999). Ion currents in smooth muscle cells from human small bronchioles: presence of an inward rectifier K+ current and three types of large conductance K+ channel. Exp Physiol 84: 835–846.

Snetkov VA, Hirst SJ, Ward JP (1996). Ion channels in freshly isolated and cultured human bronchial smooth muscle cells. Exp Physiol 81: 791–804.

Stieber J, Stöckl G, Herrmann S, Hassfurth B, Hofmann F (2005). Functional expression of the human HCN3 channel. J Biol Chem 280: 34635–34643.

Stieber J, Wieland K, Stöckl G, Ludwig A, Hofmann F (2006). Bradycardic and proarrhythmic properties of sinus node inhibitors. Mol Pharmacol 69: 1328–1337.

Tompkins JD, Lawrence YT, Parsons RL (2009). Enhancement of Ih, but not inhibition of IM, is a key mechanism underlying the PACAP-induced increase in excitability of guinea pig intrinsic cardiac neurons. Am J Physiol Regul Integr Comp Physiol 297: R52–R59.

Tu H, Zhang L, Tran TP, Muelleman RL, Li YL (2010). Diabetes alters protein expression of hyperpolarization-activated cyclic nucleotide-gated channel subunits in rat nodose ganglion cells. Neuroscience 165: 39–52.

Undem BJ, Weinreich D (1993). Electrophysiological properties and chemosensitivity of guinea pig nodose ganglion neurons in vitro. J Auton Nerv Syst 44: 17–33.

Vanner S, Evans RJ, Matsumoto SG, Surprenant A (1993). Potassium currents and their modulation by muscarine and substance P in neuronal cultures from adult guinea pig celiac ganglia. J Neurophysiol 69: 1632–1644.

Wang YP, Sun BY, Li Q, Dong L, Zhang GH, Grundy D *et al.* (2012). Hyperpolarization-activated cyclic nucleotide-gated cation channel subtypes differentially modulate the excitability of murine small intestinal afferents. World J Gastroenterol 18: 522–531.

Wilson JM, Coderre E, Renaud LP, Spanswick D (2002). Active and passive membrane properties of rat sympathetic preganglionic neurones innervating the adrenal medulla. J Physiol 545 (Pt 3): 945–960.

Wu X, Liao L, Liu X, Luo F, Yang T, Li C (2012). Is ZD7288 a selective blocker of hyperpolarization-activated cyclic nucleotide-gated channel currents? Channels (Austin) 6: 438–442.

Zhou YH, Sun LH, Liu ZH, Bu G, Pang XP, Sun SC *et al.* (2010). Functional impact of the hyperpolarization-activated current on the excitability of myelinated A-type vagal afferent neurons in the rat. Clin Exp Pharmacol Physiol 37: 852–861.